# Experimental demonstration and modeling of near-infrared nonlinear third-order triple-photon generation stimulated over one mode

Cite as: APL Quantum 2, 026114 (2025); doi: 10.1063/5.0254046
Submitted: 20 December 2024 • Accepted: 14 April 2025 •
Published Online: 25 April 2025

View Online Export Citation CrossMark

J. Bertrand, V. Boutou, C. Felix, D. Jegouso, and B. Boulanger[a)]

## AFFILIATIONS

Université Grenoble Alpes, CNRS, Grenoble INP, Institut Néel, 38000 Grenoble, France

[a)]Author to whom correspondence should be addressed: benoit.boulanger@neel.cnrs.fr

## ABSTRACT

Triple Photon Generation (TPG) is a third-order nonlinear optical interaction in which a photon of energy $\hbar\omega_p$ splits into three photons at $\hbar\omega_1$, $\hbar\omega_2$, and $\hbar\omega_3$, with $\hbar\omega_p = \hbar\omega_1 + \hbar\omega_2 + \hbar\omega_3$. The triplets possess different quantum signatures from those of photon pairs, with strong interest in quantum information. In the present study, we report the first experimental demonstration of TPG stimulated over one mode of the triplet, at $\hbar\omega_1$, whereas previous work on TPG concerned stimulation over two modes, at $\hbar\omega_2$ and $\hbar x\omega_3$. The nonlinear medium is a $KTiOPO_4$ crystal pumped in the picosecond regime (15 ps, 10 Hz) at $\lambda_p$ = 532 nm. The stimulation beam is emitted by a tunable optical parametric generator: the phase-matching was found at a stimulation wavelength $\lambda_1$ = 1491 nm, the other two modes of the triplet being at $\lambda_2 = \lambda_3$ = 1654 nm in orthogonal polarizations. Using superconducting nanowire single photon detectors, the measurements of the polarizations and wavelength signatures of the two generated modes are in full agreement with calculations. It has been possible to generate a total number of photons *per* pulse on modes 2 and 3 up to $2 \times 10^4$, which corresponds to the generation of $10^4$ triplets *per* pulse, or $10^5$ triplets *per* second since the repetition rate is equal to 10 Hz. We interpreted these results in the framework of a model we developed on the basis of the nonlinear momentum operator in the Heisenberg representation under the undepleted pump and stimulation approximation.

*© 2025 Author(s). All article content, except where otherwise noted, is licensed under a Creative Commons Attribution (CC BY) license (https://creativecommons.org/licenses/by/4.0/).* https://doi.org/10.1063/5.0254046

25 April 2025 13:37:18

## I. INTRODUCTION

Third-order parametric downconversion, also called triple photon generation (TPG), is a nonlinear interaction consisting in the scission of a high energy pump photon $\hbar\omega_p$ into three lower energy photons ($\hbar\omega_1$, $\hbar\omega_2$, and $\hbar\omega_3$). These three down-converted photons provide a new exotic quantum state of light that exhibits statistics going beyond the usual Gaussian statistics associated with coherent sources and optical parametric twin-photon generators. Actually, the direct simultaneous birth of three photons from a single one is, indeed, at the origin of intrinsic three-body quantum properties, such as three-particle Greenberger–Horne–Zeilinger (GHZ) quantum entanglement[1] and Wigner functions presenting quantum interferences and negativities.[2–6] It may also open new horizons in quantum information, as, for example, the generation of heralded two photon states, which can be used in a qubit amplifier or in a device independent quantum key distribution protocol.[7] The first experimental demonstration of a TPG was performed in the bi-stimulated regime,[8] where additional coherent and intense stimulation beams at $\hbar\omega_2$ and $\hbar\omega_3$ were injected in a phase-matched bulk $KTiOPO_4$ (KTP) crystal while being pumped at $\hbar\omega_p$. This bi-stimulated configuration strongly increases the conversion efficiency of the downconversion process and exhibits non-intuitive continuous variable entanglement properties: actually, the tripartite entanglement is predicted to increase with seeding field for the two- and three-mode seeding.[9] Nonetheless, the quantum properties of such a "mixed" state are difficult to implement in realistic quantum information protocols. The spontaneous TPG would offer the most interesting quantum state, but the conversion efficiency of such processes is very low, as shown by the quantum modeling in


© Author(s) 2025

the weak interaction approximation in the Heisenberg representation.[5] However, an experimental demonstration of such a process was performed in the GHz range,[10] but the optical range, in particular in the telecom range around 1500 nm, is still a challenge. With regard to this last objective, several unsuccessful attempts have been based on strategies using optical fibers[11,12] or crystal waveguides[6] in order to boost the generation efficiency. An important step in this quest is the mono-stimulated TPG, in which a single stimulation beam, i.e., over a single of the triplet, is injected in the nonlinear medium in addition to the pump beam. It is the framework of the present paper where we report the first experimental demonstration of a mono-stimulated TPG in the picosecond regime at telecom wavelengths using a phase-matched KTP crystal. Using superconducting nanowire single photon detectors (SNSPDs), the energy of the non-seeded modes $\hbar\omega_2$ and $\hbar\omega_3$ is measured and compared to a quantum model we developed on the basis of the nonlinear momentum operator in the Heisenberg representation.

## II. TPG CONFIGURATION

The mono-stimulated TPG is performed in the same nonlinear medium than that previously used for the bi-stimulated TPG:[8] it is a 1 cm-long KTP crystal cut along the x-axis of the dielectric frame (x, y, z), which allows birefringence phase-matching with the configuration of polarization described in Fig. 1.

Then, the energy conservation and momentum conservation are defined as follows:

$$\Delta E = \hbar\omega_p - \hbar\omega_1 - \hbar\omega_2 - \hbar\omega_3 = 0, \tag{1}$$

$$\overrightarrow{\Delta k}(\omega_p, \omega_1, \omega_2, \omega_3) = \frac{\omega_p}{c} n^-\left(\omega_p, \overrightarrow{u_p}\right)\overrightarrow{u_p} - \frac{\omega_1}{c} n^+\left(\omega_1, \overrightarrow{u_1}\right)\overrightarrow{u_1} - \frac{\omega_2}{c} n^-\left(\omega_2, \overrightarrow{u_2}\right)\overrightarrow{u_2} - \frac{\omega_3}{c} n^+\left(\omega_3, \overrightarrow{u_3}\right)\overrightarrow{u_3} = \vec{0}. \tag{2}$$

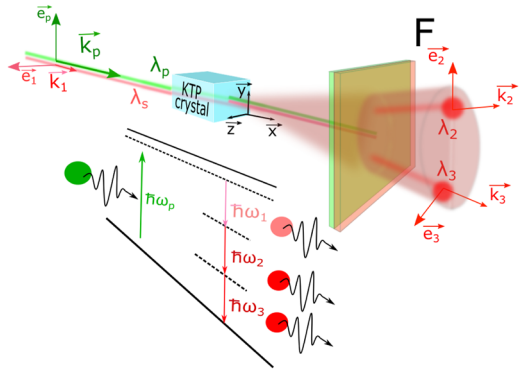


**FIG. 1.** Schematic view of a TPG stimulated over one triplet mode, at $\lambda_1$, with the two other triplet modes being at $\lambda_2 = \lambda_3$. The pump beam is at $\lambda_p$. The nonlinear medium is a phase-matched x-cut KTP crystal, where (x, y, z) is the dielectric frame. $\vec{e_p}$, $\vec{e_1}$, $\vec{e_2}$, and $\vec{e_3}$ are the unit electric field vectors of the interacting photons. $\vec{k_p}, \vec{k_1}, \vec{k_2}, \vec{k_3}$ are the corresponding wave vectors. $\chi^{(3)}_{yzzy}(\omega_p = \omega_1 + \omega_2 + \omega_3)$ is the relevant coefficient of the third-order electric susceptibility tensor of KTP. The pump and stimulation beams are filtered by a set of filters (F).

$n^-\left(\omega_m, \overrightarrow{u_m}\right)$ and $n^+\left(\omega_m, \overrightarrow{u_m}\right)$ are the eigenrefractive indices at the circular frequency $\omega_m$ for a propagation in the direction $\overrightarrow{u_m}$ of the crystal, with $m \equiv (p, 1, 2, 3)$.[13] Note that Eqs. (1) and (2) are valid for both the bi-stimulated and mono-stimulated TPG as well as for the spontaneous TPG. The full collinearity, i.e., $\overrightarrow{u_p} = \overrightarrow{u_1} = \overrightarrow{u_2} = \overrightarrow{u_3}$, is possible for both configurations of TPG, but the generation also occurs under a given level of non-collinearity in the form of a cone in the mono-stimulated case, i.e., $\overrightarrow{u_p} = \overrightarrow{u_1} \neq \overrightarrow{u_2} \neq \overrightarrow{u_3}$.

## III. EXPERIMENTAL SETUP

The experimental setup for the mono-stimulated TPG is shown in Fig. 2. A 1064-nm laser beam with a FWHM pulse duration of 15 ps at the repetition rate of 10 Hz is split into two parallel beamlines using a beam splitter (BS). The first beamline produces the pump photons at $\lambda_p = 532$ nm thanks to a second-harmonic generator based on a KTP crystal (SHG-KTP) cut at $\phi = 23°$ in the xy-plane. The second beamline is devoted to the pumping of a tunable-wavelength optical parametric generator (OPG, TOPAS Light Conversion) used for the stimulation of the TPG at $\lambda_1 = 1491$ nm.

We consider a semi-degeneracy for modes 2 and 3, i.e., $\lambda_2 = \lambda_3$, as justified in Sec. IV. In order to avoid parasitic photons, the incoming beams are spectrally cleaned by two sets of filters: F1 for the stimulation and F2 for the pump. The space and time overlap between the pump and stimulation beams is achieved using a delay line and a dichroic mirror highly reflective at 532 nm (DM). A telescope on the OPG output line is dimensioned so that the size of the stimulation beam waist *radius* in the crystal is $w_0^s = 150$ $\mu$m, which is bigger than that of the pump beam measured at $w_0^p = 82$ $\mu$m. The TPG is performed in a 1-cm-long KTP crystal (TPG-KTP). Another set of filters (F3), including notch and long-pass filters, is used to discriminate modes 2 and 3 from the other sources of light. A bandpass filter FBH1650-12 (F4) at 1650 ± 6 nm ($OD > 5$) has a broad blocking region (200–1800 nm) and is directly posted close to the injection aspheric lens to filter any residual parasitic photons from the crystal as well as pulsed ambient light. The detection is performed on modes 2 and 3 using a MoSi SNSPD from IDQuantique, cooled down to 0.8 K in a liquid helium cryostat. Because of the weakness of the signal, it is not possible to directly optimize its injection into the single mode fiber (SMF). Therefore, another parametric signal arising from the difference frequency generation between the pump and stimulation beams (1/532 − 1/1491 → 1/827 nm) is used prior to inserting F4 and F3. A polarization selector composed of a Glan–Taylor (GT) prism and a Half-Wave Plate (HWP) allows mode 2 or 3 of the triplet to be selected. The SNSPD is connected to a time-controller that is triggered by the signal from a silicon photodiode Thorlabs DET110 (PD) installed on a pump laser loss. The triggering creates a temporal filtering that removes the continuous ambient light contribution. The quantitative measurement of the triple photon flux is performed at a weak level, typically $n_{triplets} \approx 0.01$ photons per pulse, and for this, calibrated neutral densities are used. This guarantees the statistical impossibility that photons coming from two or more triplets are present in the same detected pulse. This is mandatory to avoid any problems related to the very small time-width of the optical pulse (15 ps) compared to the recovery time of the detector (30 ns). The overall detection efficiency is estimated to be about $4 \times 10^{-5}$: it takes into account the transmittance of the filters and lenses, the

25 April 2025 13:37:18


© Author(s) 2025

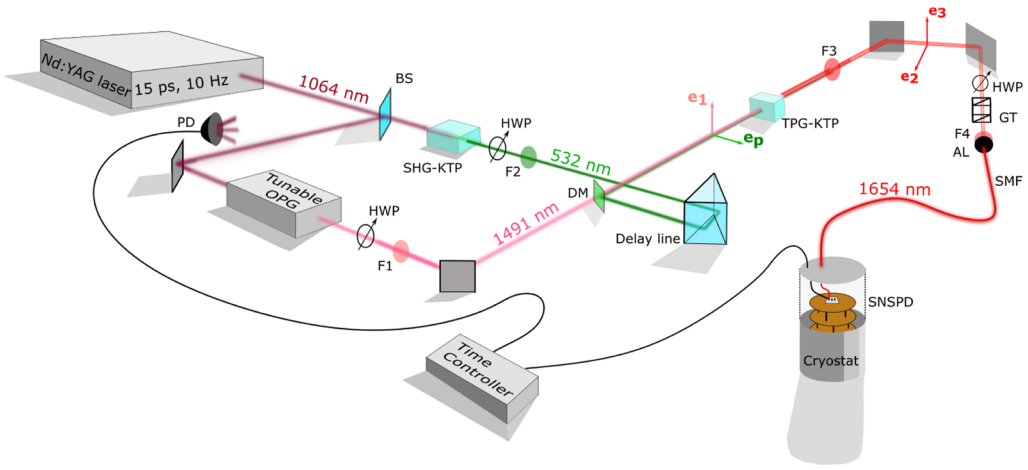


**FIG. 2.** Experimental scheme for the mono-stimulated TPG in a bulk KTP crystal using different optical components: a beam splitter (BS), an optical parametric generator (OPG), filters (F1, F2, F3, F4), a second-harmonic generator (SHG-KTP), half-wave plates (HWPs), a dichroic mirror (DM), a Glan–Taylor (GT) prism, a single-mode fiber (SMF), an aspheric lens (AL), a photodiode (PD) connected to a time controller, and a superconducting nanowire single photon detector (SNSPD) at 0.8 K in a cryostat.

coupling in the single mode fiber, as well as the detector efficiency. The extremely low value of that detection efficiency is mainly due to losses in the signal injection into the single mode fiber (SMF). Actually, the low quality of the beam profile does not fit well the SMF guided mode. Furthermore, the beam spatial jitter also reduces the average injection coefficient and increases its standard deviation.

## IV. MEASUREMENTS

### A. Wavelengths, polarizations, and divergence

We have chosen to perform the mono-stimulated TPG, for which the two non-seeded modes are at the same wavelength, i.e., $\lambda_2 = \lambda_3$, in order to be in the same configuration than for the bi-stimulated TPG studied previously and in the same direction of propagation, i.e., along the x-axis, the idea being to start from a well-mastered situation.[8] Furthermore, this phase-matching direction allows *(i)* the triplet wavelengths to be in the telecom range, which is important for quantum information applications, and *(ii)* the walk-off angle to be null, leading to a maximal spatial overlap between the interacting beams. Thus, a careful phase-matching investigation has been carried out in the bi-stimulated case, which also allowed us to select the relevant dispersion equations of the refractive indices required for the quantum model developed in Sec. V. For that purpose, the OPG has been tuned from $\lambda_2 = \lambda_3 = 1600$ nm to $\lambda_2 = \lambda_3 = 2000$ nm and the signal at $\lambda_1$ has been collected on a spectrometer. The measurement was investigated for different angles of propagation $\theta$ contained in the xz-plane by rotating the crystal. The result is shown in Fig. 3.

The experimental phase-matching wavelengths are in good agreement with the calculation using Eq. (2) and the Sellmeier equations of Ref. 14. For the following, the mono-stimulated TPG will be performed along the x-axis ($\theta = 90°$) with the following set of wavelengths and polarizations: ($\lambda_p = 532$ nm, $y-polarization$); ($\lambda_1 = 1491$ nm, $z-polarization$); ($\lambda_2 = \lambda_3 = 1654$ nm, $y-$ *and* $z-polarizations$). Then, the corresponding effective coefficient is $\chi^{(3)}_{yzzy}(1654\text{ nm}) = 7.8 \cdot 10^{-22}$ m$^2$ V$^{-2}$ deduced by using Miller's rule from $\chi^{(3)}_{yzzy}(539\text{ nm}) = 14.6 \cdot 10^{-22}$ m$^2$ V$^{-2}$ measured in a previous study.[15] Note that the filters described in Sec. III allowed us to completely cut all the possible parasitic second-order effects that can occur, i.e., spontaneous parametric downconversion (SPDC) as well as sum- or difference-frequency generations involving the pump and stimulation fields.

A clear signature of phase-matching for the mono-stimulated TPG is shown in Fig. 4, where the number of generated photons in modes 2 and 3 is plotted as a function of the detuning of the polarization angle of the pump as well as of the signal. Figure 4 well shows

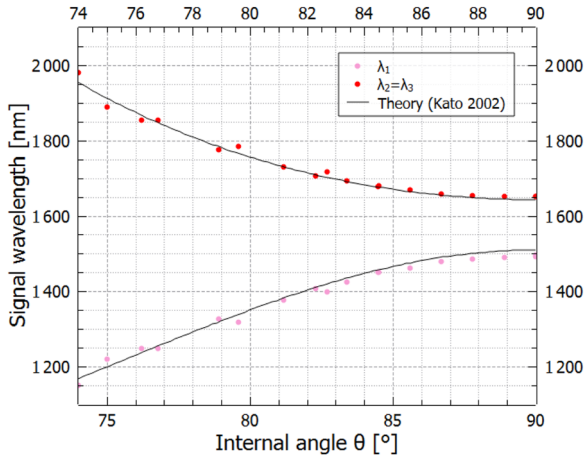


**FIG. 3.** Measured and calculated phase-matching wavelengths of the bi-stimulated TPG in the xz-plane of KTP pumped at $\lambda_p = 532$ nm as a function of the internal angle (inside the crystal) of spherical coordinate $\theta$ of the TPG phase-matching direction ($\theta = 0°$ corresponds to the z-axis and $\theta = 90°$ corresponds to the x-axis).

25 April 2025 13:37:18


© Author(s) 2025

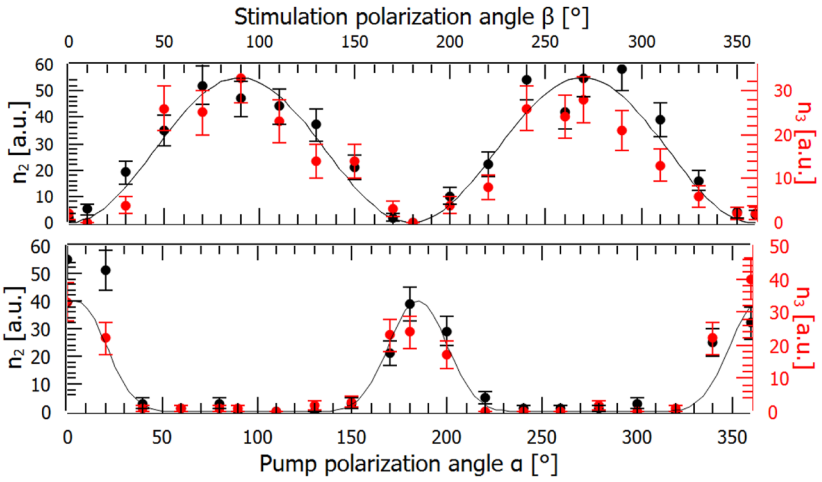


**FIG. 4.** Number of photons $n_2$ and $n_3$ in modes 2 and 3 as a function of the polarizations of the pump and stimulation angles ($\alpha$) and ($\beta$), respectively. 0° (resp. 90°) corresponds to the y-axis (resp. z-axis) of the dielectric frame of the KTP crystal. The pump and stimulation energies are $E_p$ = 26 $\mu$J and $E_s$ = 21 $\mu$J, respectively.

that the signal at $\lambda_2 = \lambda_3$ drops to 0 when the phase-matching polarization conditions are switched off, i.e., $\lambda_p$ polarized along the z-axis or $\lambda_1$ polarized along the y-axis, while it reaches a maximum when *the* phase matching conditions are switched on, i.e., $\lambda_p$ polarized along the y-axis and $\lambda_1$ polarized along the y-axis.

By using several bandpass filters, we determined that the peak wavelengths of modes 2 and 3, which correspond to the collinear contribution, i.e., $\vec{u}_p = \vec{u}_1 = \vec{u}_2 = \vec{u}_3$ in Eq. (2), are $\lambda_2 = \lambda_3 = 1654$ nm as expected.

We also measured the divergency of the pump, stimulation, and generated beam from the knife method, and we found clear evidence of the generation over a cone. Actually, the divergence of modes 2 and 3 is 12.0 mrad, which is one order of magnitude higher than for the pump (2.1 mrad) and the stimulation (4.7 mrad).

### B. Number of photons *per* pulse

Figure 5 shows the number of photons *per* pulse on modes 2 and 3 as a function of the stimulation energy ranging from 62 nJ to 21 $\mu$J and for a fixed pump energy $E_p$ = 26 $\mu$J. The energies are controlled by calibrated neutral densities. Figure 5 shows a linear behavior, which will be interpreted in Sec. V. It has been possible to generate a total number of photons *per* pulse on modes 2 and 3, i.e., $n_2 + n_3$, up to $2 \times 10^4$. That corresponds to the generation of $n_{triplets} = 10^4$ *per* pulse, which gives $10^5$ triplets *per* second since the repetition rate is equal to 10 Hz. The corresponding quantum efficiencies are $\eta = \frac{n_{triplets}}{n_p} = 0.8 \times 10^{-11}$ and $\eta/n_1 = \frac{n_{triplets}}{n_p n_1} = 3.1 \times 10^{-24}$ Hz$^{-1}$, where $n_p$ and $n_1$ are the numbers of pump and stimulation photons *per* pulse.

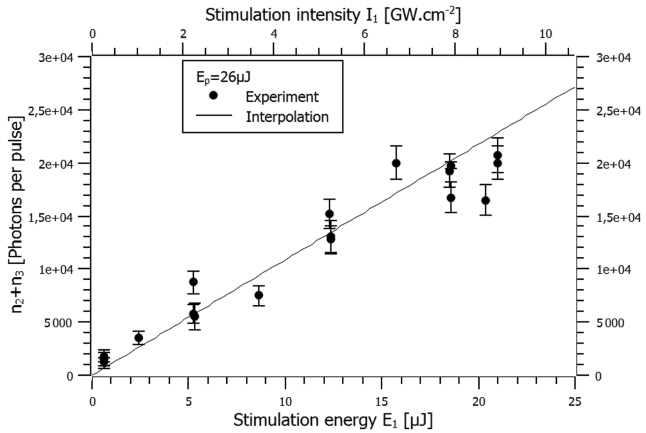


**FIG. 5.** Measurements of the number of photons on modes 2 and 3 generated by the mono-stimulated TPG in a 1-cm-long KTP crystal as a function of the stimulation energy/intensity at a given pump energy of $E_p$ = 26 $\mu$J.

## V. MODELING

We used a model in the Heisenberg representation based on the nonlinear momentum operator.[5,16,17] The propagation of the electromagnetic field in a nonlinear medium is then described by the following equation:

$$\frac{\partial a_j(\omega, Z)}{\partial Z} = -\frac{i}{\hbar}\left[a_j(\omega, Z), G_{nl}^{(3)}\right], \tag{3}$$

where $G_{nl}^{(3)}$ is the third-order nonlinear momentum operator and Z is the space coordinate along the direction of propagation. The quantum fields are described in terms of space dependent spectral mode operators $a_j(\omega, Z)$, with $j = (p, 1, 2, 3)$,[16,18] and the nonlinear process is considered as collinear, which means that Eq. (2) is reduced to a scalar equation, i.e.,

$$\Delta k(\omega_p, \omega_1, \omega_2, \omega_3) = \frac{\omega_p}{c} n_y(\omega_p, \vec{u}) - \frac{\omega_1}{c} n_z(\omega_1, \vec{u}) - \frac{\omega_2}{c} n_y(\omega_2, \vec{u}) - \frac{\omega_3}{c} n_z(\omega_3, \vec{u}) = 0, \tag{4}$$

where $\vec{u}$ is collinear to the x-axis of KTP in the present study so that $n^- = n_y$ and $n^+ = n_z$.

A single collinearly propagating spatial mode of the electromagnetic field is then considered, keeping the same logic as in Ref. 16, which gives

$$E(t, Z) = i \int_0^{+\infty} d\omega \sqrt{\frac{\hbar\omega}{4\pi\varepsilon_0 S}} a(\omega, Z) e^{-i\omega\left(t - \frac{Z}{c}\right)} + H \cdot C. \tag{5}$$

25 April 2025 13:37:18


© Author(s) 2025

This description of a 1D electromagnetic field propagating along a single spatial direction is obtained by introducing the $S$ area parameter. This area is defined by the cavity size in the two other spatial directions.[18] The nonlinear momentum model was developed from this 1D electromagnetic field formalism for both second-order and third-order spontaneous parametric downconversions.[5,16,17] The mono-stimulated TPG was partially described,[5] the pump field being assumed to be intense and non-depleted, so that the associated annihilation operator $a_p(\omega, Z)$ is well modeled by a classical spectral amplitude $A_p(\omega, Z=0)$ such that $|A_p(\omega, Z=0)|^2 = n_p(\omega, Z=0)$. The number of pump photons is then given by $\int_\omega |A_p(\omega, Z=0)|^2 d\omega = n_p(0)$, where $n_p(0)$ is expressed in photon flux unit. Moreover, regarding the weakness of the magnitude of $\chi^{(3)}$, an approximation of weak coupling was made, expressed as $|\Gamma A_p| \ll 1$, where $\Gamma$ is proportional to $\chi^{(3)}$.[5] The expressions of the field operators $a_1(\omega, Z)$, $a_2(\omega, Z)$, and $a_3(\omega, Z)$ are calculated by solving the space propagation equation (3).

Here, we derived the third-order nonlinear momentum operator in the case of the mono-stimulated TPG in the general case, i.e., without the weak-coupling approximation. The stimulated mode, i.e., mode 1 in our case without loss of generality, is assumed to be intense and non-depleted so that $a_1(\omega, Z) = a_1(\omega, Z=0) = A_1(\omega, Z=0)$, where $A_1(\omega, Z=0)$ is the spectral amplitude of mode 1 at the entrance of the crystal. Under these conditions, the third-order nonlinear momentum operator is expressed as follows:

$$G_{nl}^{(3)}(Z) \approx \int_0^{+\infty} d\omega_p \int_0^{+\infty} d\omega_1 \int_0^{+\infty} d\omega_2 \hbar\Gamma \times (\omega_p, \omega_1, \omega_2)\big(A_s(\omega_1, Z=0) a_2(\omega_2, Z) a_3(\omega_p - \omega_1 - \omega_2, Z) \breve{A}_p^T(\omega_p, Z=0) e^{-i\Delta k(\omega_p, \omega_1, \omega_2) Z} + H \cdot C \cdot \big). \quad (6)$$

From Eqs. (3)–(5), we obtain the photon-flux spectral densities, i.e., the number of photons *per* pulse *per* Hz, on modes 2 and 3,

$$n_2(\omega, Z) = n_3(\omega_p - \omega_1 - \omega, Z) = \begin{cases} 2\pi \dfrac{I_1(0) I_p(0) f^{(3)}(\omega) \left(\chi^{(3)}\right)^2}{\left|C^{(3)}(\omega)\right|} \sin^2\left(\sqrt{\left|C^{(3)}(\omega)\right|} Z\right) \\ if \quad C^{(3)}(\omega) < 0, \\ 2\pi \dfrac{I_1(0) I_p(0) f^{(3)}(\omega) \left(\chi^{(3)}\right)^2}{C^{(3)}(\omega)} \sinh^2\left(\sqrt{C^{(3)}(\omega)} Z\right) \\ if \quad C^{(3)}(\omega) > 0. \end{cases} \quad (7)$$

Here, $I_p(0)$ and $I_1(0)$ are the pump and stimulation intensities at the entrance of the crystal, respectively, and the quantities $C^{(3)}(\omega)$ and $f^{(3)}(\omega)$ are defined by

$$C^{(3)}(\omega) = 4\pi^2 I_1(0) I_p(0) f^{(3)}(\omega) \left(\chi^{(3)}\right)^2 - \frac{\Delta k(\omega)^2}{4}, \quad (8)$$

$$f^{(3)}(\omega) = \frac{1}{\left(8\pi c^2 \varepsilon_0\right)^2} \frac{\omega(\omega_p - \omega_1 - \omega)}{n_z(\omega_1) n_y(\omega) n_z(\omega_p - \omega_1 - \omega) n_y(\omega_p)}. \quad (9)$$

It was assumed for the above-mentioned calculations that the spectral bandwidths of modes 2 and 3 are wider than both the pump and stimulation spectral bandwidths so that Eq. (4) writes $\Delta k(\omega_p, \omega_1, \omega_2) = \frac{\omega_p}{c} n_y(\omega_p) - \frac{\omega_s}{c} n_z(\omega_1) - \frac{\omega_2}{c} n_y(\omega_2) - \frac{\omega_p - \omega_1 - \omega_2}{c} n_z(\omega_p - \omega_1 - \omega_2) \approx \Delta k(\omega_2) \equiv \Delta k(\omega)$ since $\omega_2$ is taken equal to $\omega$. Furthermore, the third-order electric susceptibility $\chi^{(3)}$ has to be taken equal to $\chi^{(3)}_{yzzy}$, as defined in Sec. IV.

Equation (7) shows that the mono-stimulated TPG under the undepleted pump and stimulation exhibits two regimes: the weak coupling when $C^{(3)}(\omega) < 0$, i.e., for $4\pi^2 I_1(0) I_p(0) f^{(3)}(\omega) \left(\chi^{(3)}\right)^2 \ll \frac{\Delta k(\omega)^2}{4}$, and the strong coupling when $C^{(3)}(\omega) > 0$, i.e., for $4\pi^2 I_1(0) I_p(0) f^{(3)}(\omega) \left(\chi^{(3)}\right)^2 \gg \frac{\Delta k(\omega)^2}{4}$.

The integration of Eq. (6) leads to the number of photons *per* pulse on modes 2 and 3, i.e.,

$$n_2(Z) = n_3(Z) = \int_\omega n_{2,3}(\omega, Z) d\omega. \quad (10)$$

The numerical integration of Eq. (10) leads to a linear evolution of $n_{2,3}(Z)$ with the product $I_1(0) I_p(0)$ in the weak coupling regime, while it is an exponential behavior in the strong coupling regime. From Fig. 5, it is obvious that the measured curve as a function of $I_1(0)$ for a fixed value of $I_p(0)$ is linear, which indicates that the experiments were performed in the weak coupling regime. We chose $\Delta k(\omega)$ as a fitting parameter because the modeling was performed in the collinear approximation, while the divergence relative to modes 2 and 3 is measured to be of about four times the divergence of the pump and stimulation beams, which may modify the "level" of momentum conservation. We then defined an effective phase-mismatch $\Delta k_{eff}(\omega) = \delta \Delta k(\omega)$, where $\delta$ is the fitting parameter. The interpolation is satisfying for $\delta = 2 \times 10^{-7}$ as shown in Fig. 5. It means that the effective mismatch is closer to 0 than the one given by the collinear model. An analytical expression of $n_{2,3}(Z)$ can be found thanks to the possible approximation of $\Delta k(\omega)$ as $\Delta k(\omega) \approx a + b\omega$, with $a = -3.3 \times 10^5$ rad m$^{-1}$ and $b = 2.88 \times 10^{-10}$ m$^{-1}$ Hz$^{-1}$, using the Sellmeier equations of Ref. 14. Then, from Eqs. (7)–(10),

25 April 2025 13:37:18


© Author(s) 2025

we obtain

$$n_2(Z) = n_3(Z) \approx 4\pi^2\left[f^{(3)}(\omega)\right]^2 \frac{I_p(0)I_1(0)\chi^{(3)^2}}{\delta|b|}Z. \quad (11)$$

It is the first experimental validation of the third-order nonlinear momentum operator to the best of our knowledge.

It is interesting to notice that TPG stimulated over one mode is equivalent to second-order SPDC from the flux modeling point of view.[19] This analogy can be intuited by simply considering in a first approach that $\chi^{(3)}.E$ is equivalent to $\chi^{(2)}$ from the unity point of view.

## VI. CONCLUSION

In this paper, we report the first experimental demonstration of a mono-stimulated TPG in a 1-cm x-cut KTP crystal, the proof being the linear dependence on the seeding pulse energy and the polarization dependence that is perfectly in accordance with the expected behavior. The phase matching conditions were experimentally calibrated with a bi-stimulated TPG to perform a semi-degenerate mono-stimulated TPG. Both polarization and spectral signatures are in good agreement with momentum and energy conservations. It has been possible to generate up to $n_{triplets} = 10^5\ s^{-1}$ in the telecom range, the corresponding quantum efficiencies being $\eta = \frac{n_{triplets}}{n_p} = 0.8 \times 10^{-11}$ and $\eta/n_1 = \frac{n_{triplets}}{n_p n_1} = 3.1 \times 10^{-24}\ Hz^{-1}$, where $n_p$ and $n_1$ are the numbers of pump and stimulation photons. In order to interpret these results, we developed a quantum model on the basis of the nonlinear momentum operator in the Heisenberg representation under the undepleted pump and stimulation approximation. We identified two running regimes, the so-called weak- and strong-coupling, and showed that our experiments were performed under the weak-coupling regime, with a linear behavior of the generated triplets as a function of the stimulation intensity. It is important to notice that while TPG stimulated over one mode is equivalent to a second-order SPDC regarding the flux modeling,[19] our experiments lead to triplets of photons and not pairs, even if two photons of the triplet are taken for identifying and characterizing this triplet. The agreement between experiment and theory is very good by introducing an effective phase-mismatch, which suggests improving our model by taking into account the non-collinearity of the mono-stimulated TPG. Another next step will be devoted to the quantum properties of the triplets generated by the mono-stimulated TPG. A first study could be the analysis of the three-photon coherence by observing the sum-frequency generation in a nonlinear crystal as previously done in the case of twin-photons generated by a second-order SPDC.[20] Previous calculations had shown that non-classical correlations can be put into light in this scheme. Actually, the summed-frequency fields show a fluorescence-like behavior in a very low-stimulation regime, but a classical-like behavior as soon as stimulation is high enough to be perceptible in the non-injected generated field spectrum.[5] For that purpose, it will be necessary to replace our conventional fiber by a longer one and using a clever protocol recently used for the spectrum characterization of second-order spontaneous parametric downconversion.[21]

## ACKNOWLEDGMENTS

We acknowledge the support from the Fédération QuantAlps.

## AUTHOR DECLARATIONS

### Conflict of Interest

The authors have no conflicts to disclose.

### Author Contributions

**J. Bertrand**: Formal analysis (lead); Investigation (lead); Software (lead); Writing – original draft (equal); Writing – review & editing (equal). **V. Boutou**: Conceptualization (equal); Formal analysis (lead); Investigation (lead); Methodology (equal); Supervision (equal); Writing – original draft (equal); Writing – review & editing (equal). **C. Felix**: Investigation (supporting). **D. Jegouso**: Investigation (supporting). **B. Boulanger**: Conceptualization (lead); Formal analysis (lead); Investigation (equal); Methodology (lead); Supervision (lead); Validation (lead); Writing – original draft (lead); Writing – review & editing (lead).

## DATA AVAILABILITY

The data that support the findings of this study are available from the corresponding author upon reasonable request.

## REFERENCES

[1] J.-W. Pan, D. Bouwmeester, M. Daniell, H. Weinfurter, and A. Zeilinger, "Experimental test of quantum nonlocality in three-photon Greenberger–Horne–Zeilinger entanglement," Nature **403**(6769), 515–519 (2000).

[2] K. Banaszek and P. L. Knight, "Quantum interference in three-photon down-conversion," Phys. Rev. A **55**(3), 2368–2375 (1997).

[3] F. Gravier and B. Boulanger, "Third order frequency generation in $TiO_2$ rutile and $KTiOPO_4$," Opt. Mater. **30**(1), 33–36 (2007).

[4] K. Bencheikh, F. Gravier, J. Douady, A. Levenson, and B. Boulanger, "Triple photons: A challenge in nonlinear and quantum optics," C. R. Phys. **8**(2), 206–220 (2006).

[5] A. Dot, A. Borne, B. Boulanger, K. Bencheikh, and J. A. Levenson, "Quantum theory analysis of triple photons generated by a $\chi^{(3)}$ process," Phys. Rev. A **85**(2), 023809 (2012).

[6] K. Bencheikh, M. F. B. Cenni, E. Oudot, V. Boutou, C. Félix, J. C. Prades, A. Vernay, J. Bertrand, F. Bassignot, M. Chauvet, F. Bussières, H. Zbinden, A. Levenson, and B. Boulanger, "Demonstrating quantum properties of triple photons generated by $\chi^3$ processes," Eur. Phys. J. D **76**(10), 186 (2022).

[7] J. Kołodyński, A. Máttar, P. Skrzypczyk, E. Woodhead, D. Cavalcanti, K. Banaszek, and A. Acín, "Device-independent quantum key distribution with single-photon sources," Quantum **4**, 260 (2020).

[8] J. Douady and B. Boulanger, "Experimental demonstration of a pure third-order optical parametric downconversion process," Opt. Lett. **29**(23), 2794–2796 (2004).

[9] E. A. R. González, A. Borne, B. Boulanger, J. A. Levenson, and K. Bencheikh, "Continuous-variable triple-photon states quantum entanglement," Phys. Rev. Lett. **120**(4), 043601 (2018).

[10] C. W. S. Chang, C. Sabín, P. Forn-Díaz, F. Quijandría, A. M. Vadiraj, I. Nsanzineza, G. Johansson, and C. M. Wilson, "Observation of three-photon spontaneous parametric down-conversion in a superconducting parametric cavity," Phys. Rev. X **10**, 011011 (2020).

25 April 2025 13:37:18


© Author(s) 2025

[11] M. Corona, K. Garay-Palmett, and A. B. U'Ren, "Experimental proposal for the generation of entangled photon triplets by third-order spontaneous parametric downconversion in optical fibers," Opt. Lett. **36**(2), 190–192 (2011).
[12] M. V. Chekhova, A. Cavanna, M. Taheri, C. Okoth, X. Jiang, N. Joly, and P. St. J. Russell, "Photonic crystal fibers for generating three-photon states," in *Conference on Lasers and Electro-Optics (2017)* (Optica Publishing Group, 2017), p. JM4E.5.
[13] B. Boulanger and J. Zyss, "Nonlinear optical properties," in *International Tables for Crystallography, Vol. D*, 1st ed., edited by A. Authier (International Union of Crystallography, Chester, 2006), pp. 178–219.
[14] K. Kato and E. Takaoka, "Sellmeier and thermo-optic dispersion formulas for KTP," Appl. Opt. **41**(24), 5040–5044 (2002).
[15] B. Boulanger, I. Rousseau, G. Marnier, I. Rousseau, and G. Marnier, "Cubic optical nonlinearity of," J. Phys. B: At., Mol. Opt. Phys. **32**, 475–488 (1999).
[16] B. Dayan, "Theory of two-photon interactions with broadband down-converted light and entangled photons," Phys. Rev. A **76**, 043813 (2007).
[17] B. Huttner, S. Serulnik, and Y. Ben-Aryeh, "Quantum analysis of light propagation in a parametric amplifier," Phys. Rev. A **42**(9), 5594–5600 (1990).
[18] K. J. Blow *et al.*, "Continuum fields in quantum optics," Phys. Rev. A **42**(7), 4102–4114 (1990).
[19] C. Okoth, A. Cavanna, N. Y. Joly, and M. V. Chekhova, "Seeded and unseeded high-order parametric down-conversion," Phys. Rev. A **99**, 043809 (2019).
[20] I. Abram, R. K. Raj, J. L. Oudar, and G. Dolique, "Direct observation of the second-order coherence of parametrically generated light," Phys. Rev. Lett. **57**(20), 2516–2519 (1986).
[21] N. J. Sorensen, V. Sultanov, and M. V. Chekhova, "A simple model for entangled photon generation in resonant structures," Opt. Express **33**(6), 13946–13960 (2025).

25 April 2025 13:37:18


© Author(s) 2025